RSC Advances

PAPER

View Article Online
View Journal | View Issue

Cite this: *RSC Adv.*, 2019, **9**, 8943

A ratiometric fluorescent probe for detection of exogenous mitochondrial SO_2 based on a FRET mechanism†

Zhiyang Xu, Zhen Chen, Aikun Liu, Ruixue Ji, Xiaoqun Cao and Yanqing Ge *

Received 17th December 2018
Accepted 12th March 2019

DOI: 10.1039/c8ra10328c

rsc.li/rsc-advances

A novel imidazo[1,5-*a*]pyridine-hemicyanine based ratiometric fluorescent probe for detection of mitochondrial SO_2 was designed and synthesized. The probe is based on a fluorescence resonance energy transfer (FRET) mechanism. It exhibits high selectivity and sensitivity towards SO_3^{2-} with a fast response time (3 min) and detection limit of 0.13 μM. Further, it showed low cytotoxicity and was successfully applied to image exogenous mitochondrial SO_2 in cells.

Introduction

Sulfur dioxide (SO_2), which used to be considered as a toxic environmental pollutant, is now considered to be a new possible signal molecule following nitric oxide, carbon monoxide and hydrogen sulfide.[1–4] Cancers, neurological disorders and cardiovascular diseases could be caused by high exogenous SO_2 levels. As exogenous SO_2 is produced *via* oxidation of some sulphur-containing amino acids and hydrogen sulfide in mitochondria,[5,6] it is extremely important to develop selective, sensitive and rapid methods for SO_2 detection in mitochondria.

When hydrated in aqueous media, SO_2 can be transformed into its derivatives bisulfite (HSO_3^-) and sulfite (SO_3^{2-}). Therefore, methods for the detection of HSO_3^-/SO_3^{2-} such as electrochemistry, chromatography, titration and capillary electrophoresis have been developed.[7–10] However, those methods can not realize imaging in cells.

Since the first sulfite fluorescent probe was reported by Chang group in 2010,[11] numerous probes based on nucleophilic reactions with aldehydes, Michael additions, dequenching of levulinate and coordinative interactions have been developed in recent years.[12–29] Despite the remarkable progress achieved, limitations such as long detection times and poor water solubility still remain. More importantly, those intensity-based probes are susceptible to factors like external environment, substrate concentration and instrument sensitivity.

Ratiometric fluorescent probes are more advantageous than intensity-based ones. Förster resonance energy transfer (FRET) mechanism is most widely used to construct well-performing ratiometric probes.[30–32] To date, some well-behaved ratiometric fluorescent probes for SO_2 derivatives have been developed.[33–36] However, there is great room for improvement since these probes are still subject to some drawbacks such as unsatisfactory detection limits, long response time, and poor selectivity over H_2S. Recently, we successfully synthesized the imidazole[1,5-*a*]pyridine *via* a tandem reaction.[37–39] Some fluorescent probes based on this new fluorophore for Cu^{2+}, and Hg^{2+} have been constructed subsequently.[40,41] Continuing our efforts to search for new fluorophore and extend their applications,[42–53] herein, we report a new FRET platform for the rapid detection of SO_2. Imidazole[1,5-*a*]pyridine was selected as donor, hemicyanine dyad as receptor, and piperazine as connection unit. The probe **IPIN-SO$_2$** can detect SO_3^{2-} rapidly (3 min) and sensitively in a wide pH range of 5–10. More importantly, **IPIN-SO$_2$** can be used for imaging exogenous mitochondrial SO_2 in cells.

Experimental

Materials and apparatus

UV-vis spectra were recorded on a U-2600 UV-vis spectrometer (Hitachi) and fluorescence spectra were recorded on a RF-5301PC luminescence spectrophotometer (Shimadzu) at room temperature. ^{1}H NMR and ^{13}C NMR spectra were measured on a Bruker Avance 400 (400 MHz) spectrometer ($CDCl_3$ as solvent and tetramethylsilane (TMS) as an internal standard). HRMS spectra were recorded on a Q-TOF6510 spectrograph (Agilent). Nikon fluorescence inverted microscope (Ti 2-U) was used to record cell imaging. All reagents and solvents were purchased from commercial sources and used without further purification. Metal ion solution was prepared by dissolving the deionized water with metal chloride as raw material. The anionic solution was prepared by dissolving sodium containing compounds into deionized water. Deionized water was used in the whole absorption and fluorescence detection process.

School of Chemistry and Pharmaceutical Engineering, Taishan Medical University, Tai'an 271000, PR China. E-mail: geyanqing2016@126.com; Tel: +86-538-6229741

† Electronic supplementary information (ESI) available: ^{1}H NMR, ^{13}C NMR and MS spectra of probe, and additional cell images. See DOI: 10.1039/c8ra10328c

Cell culture and imaging

Brain glioma cells were cultured in RPMI-1640 containing 10% bovine serum in a 5% CO_2/95% air incubator at 37 °C. For cell imaging experiments, the growth medium was removed and replaced by RPMI-1640 without CS. The cells were incubated in a 1 μM **IPIN-SO$_2$** incubator at 37 °C and 5% CO_2/95% air for 30 minutes. The cells were washed with PBS three times and cell images were obtained *via* an inverted fluorescence microscope from Ti 2-U (Nikon, ECLIPSE, equipped with FRET system, Mercury lamp light source). For the probe, the excitation light source is 395/25 nm and the emission collected through filter is 605/55 nm and 460/50 nm. The colocalization experiments have been carried out through Laser Scanning Confocal Microscope (FV1000, Olympus). For the probe, the excitation light source is 405 nm and the emission collected is 560–620 nm. For the MitoTracker@ Deep Red, the excitation light source is 633 nm and the emission collected through filter is 650–700 nm.

Synthesis

Synthesis of compound 3. Compound **1** and **2** were synthesized according to the literature.[5]

Compound **1** (315 mg, 1 mmol) was dissolved in ethanol (15 mL), then compound **2** (190 mg, 1 mmol) was added, and 3 drops of piperidine were added. After heating and refluxing for 12 hours, the solvent was removed under reduced pressure. A deep red solid was obtained which was used for the next step without further purification.

Synthesis of the probe IPIN-SO$_2$. Compound **4** were synthesized according to the literature.[33]

Compound **4** (253 mg, 1 mmol) was added to 30 mL dichloromethane and then DMAP (183 mg, 1.5 mmol) and EDC (288 mg, 1.5 mmol) were added. After stirring at room temperature for half an hour, compound **3** (488 mg, 1 mmol) was added and stirred for 12 hours at room temperature. Then the solvent was removed under reduced pressure to afford crude compound **IPIN-SO$_2$**, which was purified on a silica gel column (C_2H_5OH : CH_2Cl_2 = 1 : 100; yields: 68.9%). ^{1}H NMR (400 MHz, $CDCl_3$) δ 8.20 (d, J = 8.0 Hz, 2H), 8.09 (d, J = 12.0 Hz, 1H), 7.76 (d, J = 8.0 Hz, 1H), 7.58–7.50 (m, 7H), 7.02 (d, J = 8.0 Hz, 2H), 6.72 (d, J = 8.0 Hz, 1H), 4.86 (q, J = 8.0 Hz, 2H), 3.86 (s, 4H), 3.66 (s, 4H), 2.97 (t, J = 8.0 Hz, 2H), 1.81 (m, 6H), 1.60 (m, 5H), 1.44 (m, 2H), 0.97 (t, J = 8.0 Hz, 3H). ^{13}C NMR (100 MHz, $CDCl_3$) δ 179.3, 167.6, 154.9, 154.6, 142.6, 140.6, 138.7, 135.2, 129.5, 128.5, 124.1, 122.6, 120.9, 117.9, 114.2, 113.4, 112.3, 106.8, 51.4, 46.7, 44.5, 42.9, 29.0, 27.6, 26.3, 22.5, 22.0, 14.0, 13.8. HRMS: ([M]$^+$); calcd for $C_{36}H_{41}ClN_5O$: 594.2994; found: 594.3003.

Results and discussion

Synthesis of the probe IPIN-SO$_2$

The synthetic route of probe **IPIN-SO$_2$** is shown in Scheme 1. Probe **IPIN-SO$_2$** was obtained as deep purple solid powder in 89.5% yield through classical condensation of compound **3** and compound **4**. The probe **IPIN-SO$_2$** was characterized by ^{1}H NMR, ^{13}C NMR and HRMS.

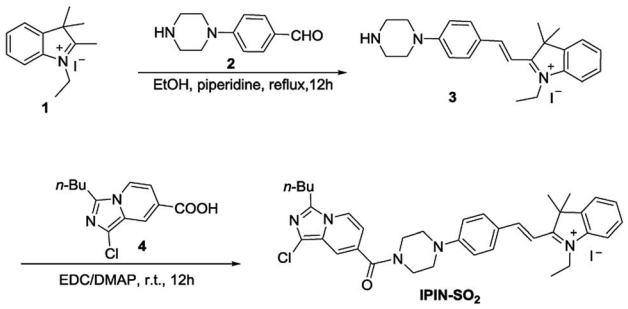

Scheme 1 Synthesis of probe IPIN-SO$_2$.

UV-vis and fluorescence spectra response of IPIN-SO$_2$

As shown in Fig. 1, **IPIN-SO$_2$** is more selective to SO_3^{2-} compared with other competitive ions, which do not cause any significant absorption changes in the visible region, which can be used as a "naked eye" chemical colorimeter. When added 10 equiv. SO_3^{2-}, the solution was obviously lighter from pink (Fig. 1, inset).

The interaction between **IPIN-SO$_2$** and SO_3^{2-} was further studied by UV-vis spectroscopic titration in 0.1 M PBS (pH = 7.4) buffer solution. **IPIN-SO$_2$** showed characteristic absorption at 500 nm. However, when the sulfite was added to the **IPIN-SO$_2$** solution, the absorption peak at 500 nm decreased rapidly with the increase of sulfite concentration as shown in Fig. S1.† When 10 equiv. amount of SO_3^{2-} was added to **IPIN-SO$_2$** solution, the fluorescence intensity immediately increased at 475 nm and the fluorescence intensity at 580 nm decreased significantly. By contrast, the other competitive cations did not cause any significant fluorescence changes, indicating that **IPIN-SO$_2$** has a better selectivity for SO_3^{2-} in the fluorescence spectrum as shown in Fig. 2.

As shown in Fig. 3, the fluorescence titration process of **IPIN-SO$_2$** was recorded. In **IPIN-SO$_2$** aqueous solution, with the

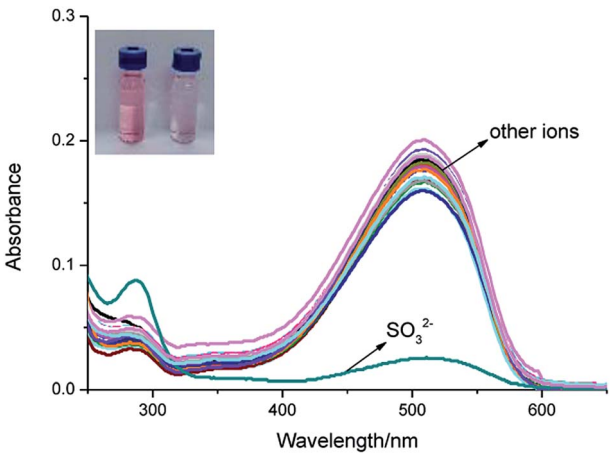

Fig. 1 Ultraviolet absorption spectra of IPIN-SO$_2$ (10 μM) in 0.1 M PBS (pH = 7.4) buffer solution with addition of 100 μM of various species (SO_3^{2-}, AcO^-, Br^-, $H_2PO_4^-$, Cl^-, CO_3^{2-}, HCO_3^-, F^-, HPO_4^{2-}, I^-, NO_2^-, NO_3^-, $S_2O_3^{2-}$, SO_4^{2-}, HS^-, Fe^{3+}, Ca^{2+}, Cu^{2+}, K^+, Na^+, Zn^{2+}), GSH (glutathione), Hcy (homocysteine), Cys (cysteine).

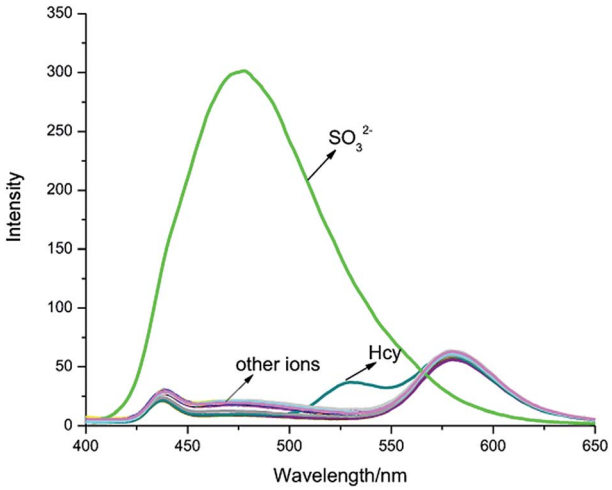

Fig. 2 Fluorescence spectra of **IPIN-SO_2** (10 μM) in 0.1 M PBS (pH = 7.4) buffer solution with addition of 100 μM of various species (λ_{ex} = 380 nm).

increase of SO_3^{2-} concentration, the fluorescence intensity increases at 475 nm and decreases at 580 nm, and the two emission peaks can be well separated (105 nm). The results show that the developed FRET system can effectively avoid the overlap of emission spectra and ensure the high resolution and accuracy of the determination. Moreover, when SO_3^{2-} concentration increased from 0 μM to 30 μM, the fluorescence intensity ratio increased from 0.29 to 12.78, about 44 times. When SO_3^{2-} concentration was in the range of 1.5–4.0 μM, there was a good linear relationship as shown in Fig. S2.†

According to LOD = $3\sigma/k$ (σ is the standard deviation of ten blank solutions and k is the slope of the linear calibration plot between the fluorescence intensity and the concentration of SO_3^{2-}), the detection limit was as low as 0.13 μM.

In addition, the interference experiments were carried out under the coexistence of various species (Fig. 4). Background ions did not interfere with fluorescence intensity. Sulfite-induced fluorescence enhancement (I_{475}/I_{580}) remained unaffected by the coexistence of other species.

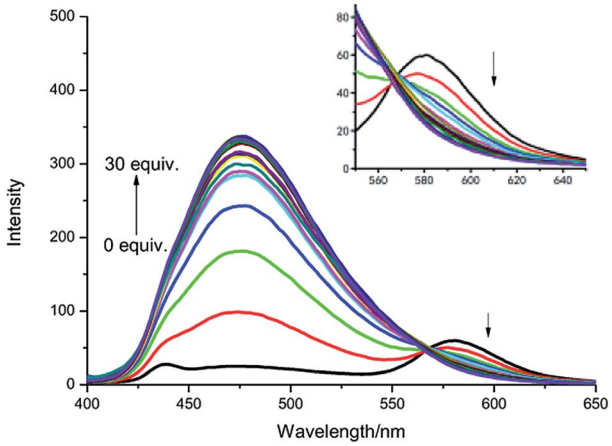

Fig. 3 Fluorescence spectra of **IPIN-SO_2** (10 μM) with the addition of SO_3^{2-} (0–30 equiv.) in 0.1 M PBS (pH = 7.4) buffer solution (λ_{ex} = 380 nm).

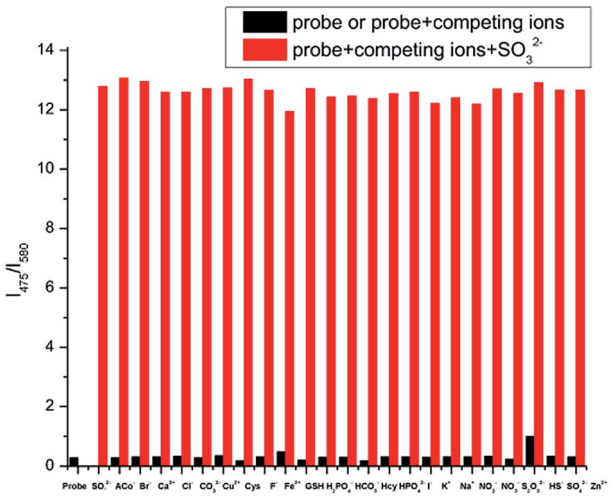

Fig. 4 Ratiometric fluorescence responses I_{475}/I_{580} of **IPIN-SO_2** (10 μM) upon the addition of 10 equiv. SO_3^{2-} in the presence of 100 μM background ions in PBS (pH = 7.4) buffer solution.

Kinetic study

In Fig. 5, the time course of fluorescence response of **IPIN-SO_2** aqueous solution with SO_3^{2-} is shown. The fluorescence intensity ratio (I_{475}/I_{580}) reached the maximum value in 3 min when 10 equiv. SO_3^{2-} was added and the fluorescence ratio of **IPIN-SO_2** almost remained unchanged with time, which indicates that **IPIN-SO_2** can be used as a fast response SO_3^{2-} probe.

Effect of pH

As shown in Fig. 6, in order to detect SO_3^{2-} efficiently and selectively, the effect of different acid concentrations on **IPIN-SO_2** was studied to find the suitable pH range. In PBS buffer solution, the fluorescence titration curves of **IPIN-SO_2** and **IPIN-SO_2** have no obvious change between pH 5.0 and 10.0 of fluorescence intensity ratio (I_{475}/I_{580}), indicating that the sensor

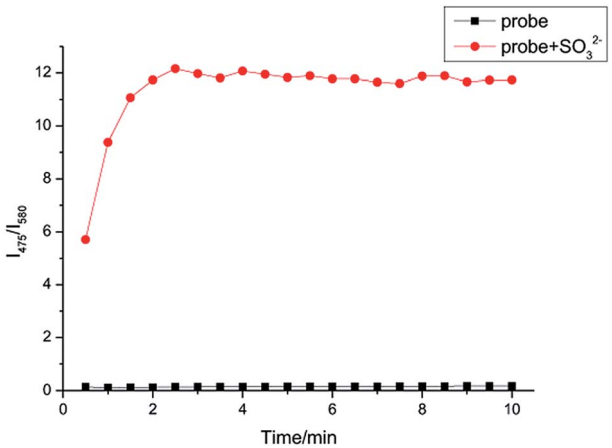

Fig. 5 Time dependent increase of **IPIN-SO_2** (10 μM) fluorescence intensities after addition of 10 equiv. SO_3^{2-} in PBS (pH = 7.4) solution (λ_{ex} = 380 nm).

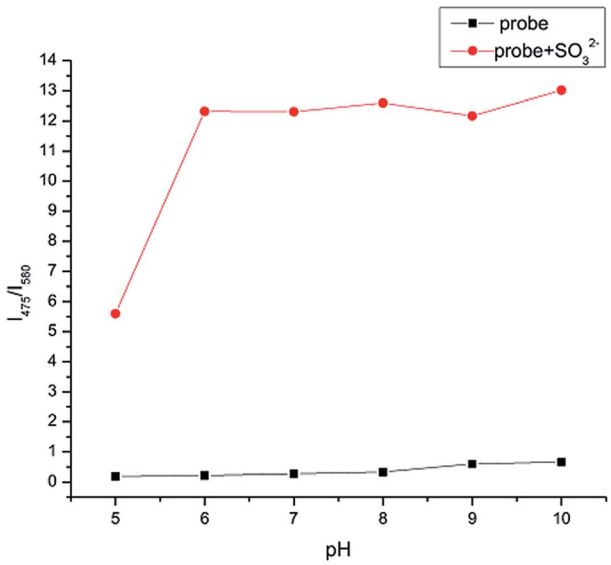

Fig. 6 Ratio of fluorescent intensities at 475 nm and 580 nm for **IPIN-SO$_2$** (10 μM) in the presence of SO_3^{2-} (10 equiv.) at varied pH values (λ_{ex} = 380 nm).

IPIN-SO$_2$ and the sensor **IPIN-SO$_2$** existing in SO_3^{2-} are stable within this pH range.

Mechanism

As shown in Scheme 2, once the **IPIN-SO$_2$** energy donor is excited, FRET will enter the hemicyanine group from the imidazole[1,5-*a*] pyridine fluorescent group, which may weaken or even quench the fluorescence of the imidazole[1,5-*a*]pyridine fluorescent group. Interruption of the p–π conjugation in the hemicyanine fluorophore results in increasing the energy of its first singlet level above that of the donor group. In addition, both the probe **IPIN-SO$_2$** and the donor can be activated at 380 nm, but the receptor cannot, which further confirms the FRET process in probe **IPIN-SO$_2$**.

To further clarify the proposed mechanism, HRMS of the reaction product was conducted. A clear mass (*m*/*z* 676.2735) of adduct appeared after the probe reacted with SO_3^{2-} (Fig. S8†).

Cell imaging

As probe **IPIN-SO$_2$** shows excellent optical response to SO_3^{2-} *in vitro*, cell imaging of **IPIN-SO$_2$** has been further studied in glioma cells. **IPIN-SO$_2$** fluorescence is stable in living cell (Fig. S3†) and cytotoxicity is negligible at 1–16 μM concentration (Fig. S4†). Because cationic cyanine dyes may accumulate in

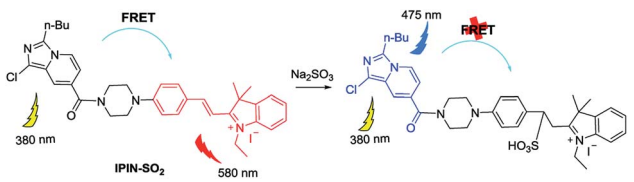

Scheme 2 Proposed sensing mechanism of **IPIN-SO$_2$** with SO_3^{2-}.

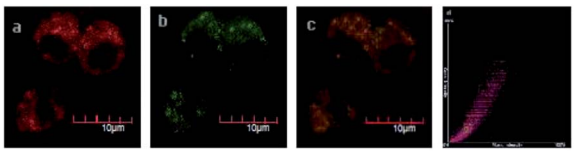

Fig. 7 Glioma cells were incubated with **IPIN-SO$_2$** (0.1 μM) for 1 h, followed by MitoTracker@ Deep Red (0.01 μM) for 0.5 h. (a) The fluorescence image of MitoTracker@ Deep Red FM. λ_{ex} = 633 nm, λ_{em} = 650–700 nm. (b) The fluorescence image of probe **IPIN-SO$_2$**. λ_{ex} = 405 nm, λ_{em} = 560–620 nm. The red fluorescence was colored as green for discrimination. (c) Merged images of (a) and (b). (d) Colocalization coefficient (Pearson's coefficient) of **IPIN-SO$_2$** and MitoTracker@ Deep Red was 0.948.

mitochondria,[54,55] colocalization assays were performed with MitoTracker@ Deep Red FM and **IPIN-SO$_2$** (Fig. 7). The fluorescence of **IPIN-SO$_2$** and MitoTracker@ Deep Red FM has a significant overlap, and the overlap coefficient is 0.948 (Fig. 7d), indicating that **IPIN-SO$_2$** was well distributed in mitochondria.

Then the probe **IPIN-SO$_2$** was applied to SO_3^{2-} imaging in living glioma cells. When the glioma cells were incubated with probe **IPIN-SO$_2$** for 1 hour, the red channel showed strong fluorescence and blue channel weak fluorescence (Fig. S5†). When incubated for 0.5 hour with different concentrations of Na_2SO_3, the cells showed enhanced fluorescence of red channel and decreased fluorescence of blue channel.

Furthermore, we studied whether the probes could be used to detect exogenous bisulfite in cells. Glioma cells were

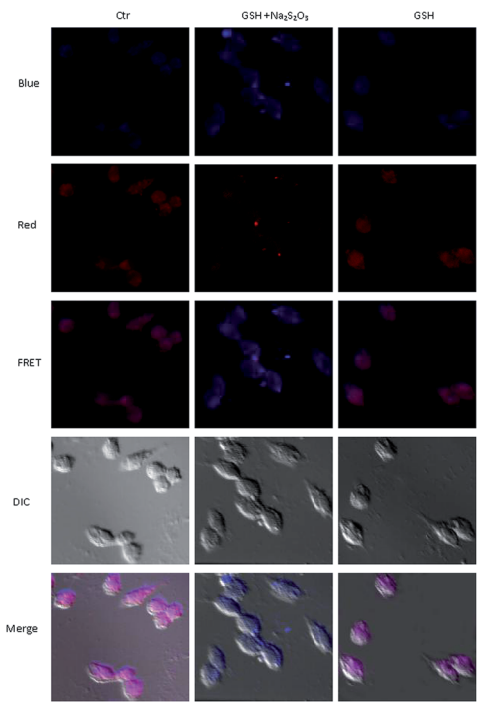

Fig. 8 The first line (vertically): glioma cells were incubated with **IPIN-SO$_2$** (0.1 μM) for 1 h; the second line: glioma cells were incubated with **IPIN-SO$_2$** (0.1 μM) for 1 h, and then with 0.5 mM GSH and 0.25 mM $Na_2S_2O_3$ for another 0.5 h; the third line: glioma cells were incubated with probe (0.1 μM) for 1 h, then with 0.5 mM GSH for 0.5 h.

incubated with probe **IPIN-SO_2** for 1 hour, washed with PBS solution three times, incubated with 0.5 mM GSH (glutathione) and 0.25 mM $Na_2S_2O_3$ for 0.5 hour, and then photographed with fluorescence inverted microscope to observe obvious fluorescence changes in glioma cells (Fig. 8). On the contrary, no significant fluorescence changes were observed when the glioma cells incubated with **IPIN-SO_2** were incubated only with GSH or $Na_2S_2O_3$. These results indicate that the probe can detect exogenous bisulfite in glioma cells.

Conclusions

In summary, a novel FRET-based ratio fluorescence probe of imidazole[1,5-*a*]pyridine substituted hemicyanines has been developed. **IPIN-SO_2** has unique selectivity and high sensitivity (detection limit 0.13 μM) for SO_3^{2-}, which can detect SO_3^{2-} rapidly (3 min) over a wide pH range of 5 to 10. It is noteworthy that the new ratio fluorescence probe avoids automatic fluorescence, severe self-quenching and fluorescence detection errors. More importantly, the probe has been successfully applied to the identification of exogenous SO_2 in mitochondria in cells.

Conflicts of interest

There are no conflicts to declare.

Acknowledgements

This work was supported by the Science Fund of Shandong Province for Excellent Young Scholars (ZR2017JL015), the Natural Science Foundation of China (21602153) and the Natural Science Foundation of Shandong Province (ZR2018LB014).

Notes and references

1 S. X. Du, H. F. Jin, D. F. Bu, X. Zhao, B. Geng, C. S. Tang and J. B. Du, *Acta Pharmacol. Sin.*, 2010, **29**, 923–930.
2 Y. F. Liang, D. Liu, T. Ochs, C. S. Tang, S. Chen, S. Q. Zhang, B. Geng, H. F. Jin and J. B. Du, *Lab. Invest.*, 2011, **91**, 12–23.
3 Z. Xu and L. Xu, *Chem. Commun.*, 2016, **47**, 1094–1119.
4 X. G. Yang, Y. B. Zhou, X. F. Zhang, S. Yang, Y. Chen, J. R. Guo, X. X. Li, Z. H. Qing and R. H. Yang, *Chem. Commun.*, 2016, **52**, 10289–10292.
5 D. P. Li, Z. Y. Wang, X. J. Cao, J. Cui, X. Wang, H. Z. Cui, J. Y. Miao and B. X. Zhao, *Chem. Commun.*, 2016, **52**, 2760–2763.
6 W. J. Zhang, T. Liu, F. J. Huo, P. Ning, X. M. Meng and C. X. Yin, *Anal. Chem.*, 2017, **89**, 8079–8083.
7 G. J. Mohr, *Chem. Commun.*, 2002, 2646–2647.
8 A. Isaac, A. J. Wain, R. G. Compton, C. Livingstone and J. Davis, *Analyst*, 2005, **130**, 1343–1344.
9 L. H. Yu, J. M. Kim and R. D. Schemid, *Anal. Chim. Acta*, 1992, **26**, 317–323.
10 S. S. Hassan, M. S. Hamza and A. H. Mohamed, *Anal. Chim. Acta*, 2006, **570**, 232–239.
11 M. G. Choi, J. Hwang, S. Eor and S. K. Chang, *Org. Lett.*, 2010, **12**, 5624–5627.
12 J. Yang, K. Li, J. T. Hou, L. L. Li, C. Y. Lu, Y. M. Xie, X. Wang and X. Q. Yu, *ACS Sens.*, 2016, **1**, 166–172.
13 J. C. Xu, J. Pan, X. M. Jiang, C. Q. Qin, L. T. Zeng, H. Zhang and J. F. Zhang, *Biosens. Bioelectron.*, 2016, **77**, 725–732.
14 W. Xu, L. T. Chai, J. Peng, D. Su, L. Yuan and Y. T. Chang, *Biomaterials*, 2015, **56**, 1–9.
15 Y. Liu, K. Li, K. X. Xie, L. L. Li, K. K. Yu, X. Wang and X. Q. Yu, *Chem. Commun.*, 2016, **52**, 3430–3433.
16 D. P. Li, X. J. Han, Z. Q. Yan, Y. Cui, J. Y. Miao and B. X. Zhao, *Dyes Pigm.*, 2018, **151**, 95–101.
17 K. Q. Xiang, S. Z. Chang, J. J. Feng, C. J. Li, W. Ming, Z. Y. Liu, Y. C. Liu, B. Z. Tian and J. L. Zhang, *Dyes Pigm.*, 2016, **134**, 190–197.
18 H. D. Li, Q. C. Yao, J. L. Fan, C. Hu, F. Xu, J. J. Du, J. Y. Wang and X. J. Peng, *Ind. Eng. Chem. Res.*, 2016, **55**, 1477–1483.
19 Y. Z. Zhu, W. Du, M. Z. Zhang, Y. Xu, L. L. Song, Q. Zhang, X. H. Tian, H. P. Zhou, J. Y. Wu and Y. P. Tian, *J. Mater. Chem. B*, 2017, **5**, 3862–3869.
20 Y. Liu, K. Li, M. Y. Wu, Y. H. Liu, Y. M. Xie and X. Q. Yu, *Chem. Commun.*, 2015, **51**, 10236–10239.
21 Y. F. Wang, Q. T. Meng, R. Zhang, H. Jia, X. H. Zhang and Z. Q. Zhang, *Org. Biomol. Chem.*, 2017, **15**, 2734–2739.
22 J. Xu, D. J. Zheng, M. M. Su, Y. C. Chen, Q. C. Jiao, Y. S. Yang and H. L. Zhu, *Org. Biomol. Chem.*, 2018, **16**, 6940–6946.
23 G. Wang, H. Chen, X. L. Chen and Y. M. Xie, *RSC Adv.*, 2016, **6**, 18662–18666.
24 Z. Chen, F. Z. Chen, Y. C. Sun, H. Liu, H. P. He, X. H. Zhang and S. F. Wang, *RSC Adv.*, 2017, **7**, 2573–2577.
25 J. Yang, K. Li, J. T. Hou, C. Y. Lu, L. L. Li, K. K. Yu and X. Q. Yu, *Sci. China: Chem.*, 2017, **60**, 793–798.
26 W. L. Wu, H. L. Ma, M. F. Huang, J. Y. Miao and B. X. Zhao, *Sens. Actuators, B*, 2017, **241**, 239–244.
27 L. J. Tang, P. He, X. M. Yan, J. Z. Sun, K. L. Zhong, S. H. Hou and Y. J. Bian, *Sens. Actuators, B*, 2017, **247**, 421–427.
28 Q. Sun, W. B. Zhang and J. H. Qian, *Talanta*, 2017, **162**, 107–113.
29 H. Huang, W. Liu, X. J. Liu, Y. Q. Kuang and J. H. Jiang, *Talanta*, 2017, **168**, 203–209.
30 L. Yuan, W. Lin, K. Zheng and S. Zhu, *Acc. Chem. Res.*, 2013, **46**, 1462–1473.
31 M. H. Lee, J. S. Kim and J. L. Sessler, *Chem. Soc. Rev.*, 2015, **44**, 4185–4191.
32 H. Zhu, J. L. Fan, B. H. Wang and X. J. Peng, *Chem. Soc. Rev.*, 2015, **44**, 4337–4366.
33 F. Chen, A. Liu, R. Ji, Z. Xu, J. Dong and Y. Ge, *Dyes Pigm.*, 2019, **165**, 212–216.
34 D. Zhang, A. Liu, R. Ji, J. Dong and Y. Ge, *Anal. Chim. Acta*, 2019, **1055**, 133–139.
35 G. Zhang, R. Ji, X. Kong, F. Ning, A. Liu, J. Cui and Y. Ge, *RSC Adv.*, 2019, **9**, 1147–1150.
36 G. Song, A. Liu, H. Jiang, R. Ji, J. Dong and Y. Ge, *Anal. Chim. Acta*, 2019, **1053**, 148–154.
37 Y. Q. Ge, B. Q. Hao, G. Y. Duan and J. W. Wang, *J. Lumin.*, 2011, **131**, 1070–1076.

38 Y. Q. Ge, T. Wang, G. Y. Duan, L. H. Dong, X. Q. Cao and J. W. Wang, *J. Fluoresc.*, 2012, **22**, 1531–1538.
39 Y. Q. Ge, J. Jia, T. Wang, H. W. Sun, G. Y. Duan and J. W. Wang, *Spectrochim. Acta, Part A*, 2014, **123**, 336–341.
40 Y. Q. Ge, R. X. Ji, S. L. Shen, X. Q. Cao and F. Y. Li, *Sens. Actuators, B*, 2017, **245**, 875–881.
41 Y. Q. Ge, X. J. Xing, A. K. Liu, R. X. Ji, S. L. Shen and X. Q. Cao, *Dyes Pigm.*, 2017, **146**, 136–142.
42 Y. Q. Ge, J. Jia, H. Yang, X. T. Tao and J. W. Wang, *Dyes Pigm.*, 2011, **88**, 344–349.
43 Y. Q. Ge, A. K. Liu, R. X. Ji, S. L. Shen and X. Q. Cao, *Sens. Actuators, B*, 2017, **251**, 410–415.
44 R. X. Ji, A. K. Liu, S. L. Shen, X. Q. Cao, F. Li and Y. Q. Ge, *RSC Adv.*, 2017, **7**, 40829–40833.
45 A. K. Liu, R. X. Ji, S. L. Shen, X. Q. Cao and Y. Q. Ge, *New J. Chem.*, 2017, **41**, 10096–10100.
46 R. X. Ji, K. Qin, Y. Zhu and Y. Q. Ge, *Tetrahedron Lett.*, 2018, **59**, 2372–2375.
47 P. L. Yan, G. Y. Duan, R. X. Ji and Y. Q. Ge, *Tetrahedron Lett.*, 2018, **59**, 2426–2429.
48 C. Wang, D. Zhang, X. Huang, P. Ding, Z. Wang, Y. Zhao and Y. Ye, *Sens. Actuators, B*, 2014, **198**, 33–40.
49 Y. Q. Ge, P. Wei, T. Wang, X. Q. Cao, D. D. Zhang and F. Y. Li, *Sens. Actuators, B*, 2018, **254**, 314–320.
50 Y. Q. Ge, A. K. Liu, J. Dong, G. Y. Duan, X. Q. Cao and F. Y. Li, *Sens. Actuators, B*, 2017, **247**, 46–52.
51 P. Zhang, H. Y. Lv, G. Y. Duan, J. Dong and Y. Q. Ge, *RSC Adv.*, 2018, **8**, 30732–30735.
52 Y. Q. Ge, X. L. Zheng, R. X. Ji, S. L. Shen and X. Q. Cao, *Anal. Chim. Acta*, 2017, **965**, 103–110.
53 X. L. Zheng, R. X. Ji, X. Q. Cao and Y. Q. Ge, *Anal. Chim. Acta*, 2017, **978**, 48–54.
54 Y. Chen, C. Zhu, Z. Yang, J. Chen, Y. He, Y. Jiao, W. He, L. Qiu, J. Cen and Z. Guo, *Angew. Chem., Int. Ed.*, 2013, **52**, 1688–1691.
55 W. Xu, Z. Zeng, J. H. Jiang, Y. T. Chang and L. Yuan, *Angew. Chem., Int. Ed.*, 2016, **55**, 13658–13699.